Heat Transfer Correlation during Gas-Cooling Process of Carbon Dioxide in a Horizontal Tube

Byung Ha Kang†, Yi Cheol Choi*, Sukhyun Kim

School of Mechanical and Automative Engineering, Kookmin University, Seoul 136-702, Korea

**Graduate School, Kookmin University, Seoul 136-702, Korea*

Key words: Carbon dioxide, Correlation, Gas-cooling, Heat transfer, Pressure drop

ABSTRACT: The characteristics of heat transfer and pressure drop have been investigated experimentally during gas-cooling process of carbon dioxide. The results of this study are useful information in the design of a heat exchanger of CO_2 refrigerator. The test section consists of 6 series of copper tube, 4.15 and 2.18 mm ID, respectively. The inlet temperature, the operating pressure, and the mass flux are varied in the range of 80~120℃, 7~10 MPa, and 400~1,900 kg/m^{2}s, respectively. The heat transfer coefficient of CO_2 is affected by temperature, inlet pressure, and mass flux of CO_2. At the maximum HTC, the temperature of CO_2 nearly accords with the psuedocritical temperature. It is found that the pressure drop is substantially affected by mass flux and inlet pressure of CO_2. The results have been compared with those of previous work. The heat transfer correlation at the gas-cooling process has been also suggested which predicts within the error of 20%.

Nomenclature

c_p : specific heat [J/(kg·K)]
D_i : inner diameter of tube [m]
D_o : outer diameter of tube [m]
G : mass flux [kg/(m^2·s)]
h : heat transfer coefficient [W/(m^2·K)]
i : specific enthalpy [J/kg]
k_{cu} : thermal conduct coefficient of copper [W/(m·K)]
L : length [m]
$\dot{m}$: mass flow rate [kg/s]
Nu : Nusselt number
P : pressure [kPa]
Pr : Prandtl number
q : heat flux [kW/(m^2·s)]
Re : Reynolds number
R_{rt} : relative roughness of tube
T : temperature [℃]

Greek symbols

ρ : Prandtl number

Subscripts

in : inlet
m : mean value
out : outlet
w : inside wall of CO_2 tube
w, o : outside wall of CO_2 tube

† Corresponding author
Tel.: +82-2-910-5053; fax: +82-2-910-4839
E-mail address: bhkang@kookmin.ac.kr

1. Introduction

Even though carbon dioxide as a refrigerant was primarily used in marine applications from 1890 to 1930, CO_2 was phased out as a refrigerant since CFCs had been developed.[1] How-

ever, the use of CFCs and HCFCs has been restricted due to ozone depletion and global warming effects by Montreal and Kyoto protocol. Recently, natural refrigerant becomes an important issue in refrigeration systems and much work has been done on refrigerant systems using natural refrigerants such as CO_2, NH_3, water, hydrocarbon and so on. Among the natural refrigerants, CO_2 has been focused on as a refrigerant because of many remarkable advantages, environmental attractiveness, non-toxicity, non-inflammability, light weight, economical price, and large refrigeration capacity. With these attractions, it has good thermal characteristics such as low surface tension and low liquid viscosity. However, it has a problem to operate in transcritical cycle because it has relatively low critical temperature, 304.21 K and high critical pressure, 7.384 MPa. It means that heat rejection occurs in supercritical region and heat absorption occurs in subcritical region.[2,3]

Many of the recent investigations of CO_2 as a refrigerant have dealt with a thermodynamic cycle analysis, which includes the critical information such as the analysis of theoretical performance and a lot of useful information for system design.[1,4] However, not much work has been carried out to measure local heat transfer coefficients and pressure drop characteristics in the process of the heat rejection.

Krasnoshckekov et al.[5] investigated heat transfer characteristics with turbulent flow in a round tube of CO_2 under cooling condition and proposed heat transfer correlation which predicted within the error of 25%. Petrov and Popov[6] and Fang et al.[7] proposed heat transfer correlation by theoretical model. Olson[8] and Pitla et al.[9] studied heat transfer characteristics during supercritical gas-cooling process. Yoon et al.[2] showed heat transfer and pressure drop characteristics during cooling process and proposed heat transfer correlation which predicted within the error of 20%. The results of heat transfer correlation are found to be different each other depending on operating conditions and tube diameter. Although these included the supercritical region, existing heat transfer correlations did not deal with critical region. Therefore, new correlation is required when a new gas cooler is proposed.

The present study is directed at estimating heat transfer coefficient and pressure drop during the subcritical and supercritical gas-cooling process of CO_2 in 4.15 mm and 2.18 mm. The new correlation on the heat transfer of CO_2 including critical region is also proposed and compared to those of previous results.

2. Experimental apparatus and methods

2.1 Experimental apparatus

The experimental apparatus for the present study has been designed and built to operate at high temperature and pressure. The tube of CO_2 is connected by high-pressure fitting. Figure 1 shows the schematic diagram of experimental apparatus. This is divided into three major loops, the CO_2 loop, the water loop for gas-cooling and the ethylene glycol/water mixture loop for subcooling of the CO_2.

The CO_2 stored in the state of compressed liquid is circulated by variable speed magnetic gear pump and passes into the preheater which is heated electrically. Then, the CO_2 inside the preheater is heated indirectly by electric heating coil. At the same time, the temperature of CO_2 is controlled in accord with the experimental condition. The pressure regulator also controls the pressure of CO_2 minutely. The flow rate of CO_2 is measured by the coriolis mass flow meter. After the flow meter, the CO_2 enters the test section and is cooled by water. After cooling process, it enters the liquid receiver and reenters the gear pump.

The test section, which is a tube-in-tube counter flow heat exchanger, is connected in 6 series, and specifications of the test sections

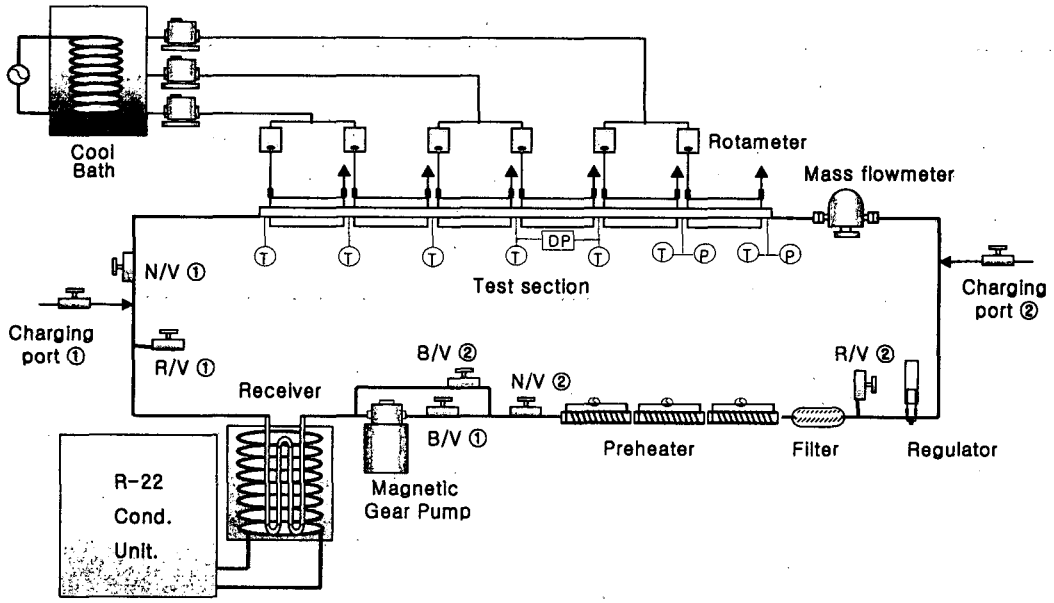

Fig. 1 Schematic diagram of experimental apparatus.

Table 1 Specifications of the test section

		Outer diameter	Inner diameter	Length	Material
Case 1	Outside	28.58	26.04	455	Copper
	Inside	6.35	4.15		
Case 2	Outside	12.7	10.5	300	Copper
	Inside	3.18	2.18		

are shown in Table 1. The inlet and outlet temperature of CO_2 and water in subsection were measured by T type thermocouples. The outside wall temperature of inner tube was measured by T type thermocouples at mid point. At the inlet of the test section, the pressure of CO_2 is gauged by the absolute pressure transducer. The pressure drop is measured by differential pressure sensors between the inlet and outlet of the first subsection and through the test section. The water for cooling the CO_2 is supplied toward subsection and flow rate is measured by rotameter.

2.2 Data reduction procedures

Energy balances of test section were checked by heat exchange rate as shown in Eq. (1). Each heat transfer coefficient of subsections was calculated by Eq. (2).

$$Q = \dot{m}_{water} c_{p,\,water} (T_{out,\,water} - T_{in,\,out}) = \dot{m}_{CO_2} (i_{out,\,CO_2} - i_{in,\,CO_2}) \quad (1)$$

$$h = \frac{q}{T_m - T_w} \quad (2)$$

The heat flux, q, was calculated by average heat transfer rate of water and CO_2 side and heat transfer area as shown in Eq. (3). T_m is the mean temperature of the inlet and outlet of CO_2, and T_w was calculated by the one dimensional equation of thermal conduction as shown in Eq. (4).

Table 2 Test conditions

Parameter	Case 1	Case 2
	4.15 mm ID	2.18 mm ID
Mass flow rate of CO_2 (kg/ms)	400, 500, 600, 700	700, 100, 1500, 1900
Inlet pressure of CO_2 (MPa)	7, 8, 9, 10	7, 8, 9, 10
Inlet temperature of CO_2 (℃)	80, 90, 100, 110	120
Mass flow rate of water (kg/s)	0.050	0.050
Inlet temperature of water (℃)	15	15

$$q = \frac{(Q_{CO_2} + Q_{water})/2}{\pi D_i L} \tag{3}$$

$$T_w = T_{w,o} + q\frac{D_i}{2k_{Cu}} \ln\left(\frac{D_o}{D_i}\right) \tag{4}$$

However, in the case 2, diameter of CO_2 tube is too small to measure the CO_2 temperature. So, the CO_2 temperature is obtained from the function of enthalpy and pressure as shown in Eq. (5).

$$T_n = f(i_n, P_n) \tag{5}$$

Here, enthalpy is calculated by inlet enthalpy and heat transfer rate as shown in Eq. (6). Pressure is calculated by inlet pressure and pressure drop as shown in Eq. (7).

$$i_n = i_{n-1} + \frac{Q_{water,n}}{\dot{m}_{CO_2}} \tag{6}$$

$$\Delta P = \frac{P_{in} - P_{out}}{n} \tag{7a}$$

$$P_n = P_{in} - \Delta P \tag{7b}$$

2.3 Test conditions

Experiments were carried out at various inlet temperatures, pressures, and mass fluxes of CO_2. The inlet temperature was adjusted 80 to 120℃, the operating pressure was set at 7, 8, 9, and 10 MPa, and the mass flux was controlled at 400, 500, 600, 700, 1,100, 1,500, 1,900 kg/m^{2}s as shown in Table 2.

3. Results and discussion

The energy balance of the test section was confirmed by Eq. (1). In the present experiments, the heat balance error of the test section is within 5%.

3.1 Heat transfer characteristics

Figure 2 shows the effects of inlet temperature of CO_2 on HTC (heat transfer coefficient) at a fixed mass flux. In this figure, it is found that HTC rarely depends on inlet temperature of CO_2. During the gas-cooling process, the HTC of CO_2 gradually increases with a decrease in the operating temperature. Then, the HTC decreases after reaching the maximum value nearby the critical region. The HTC variations according to the temperature have a

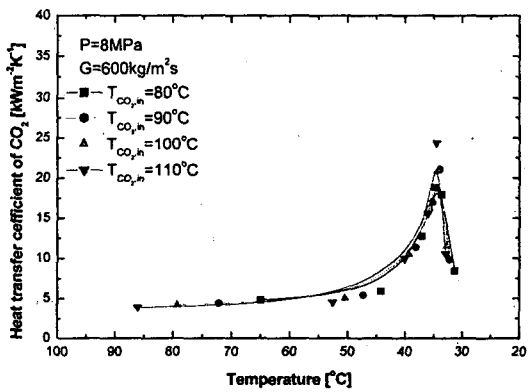

Fig. 2 Effect of inlet temperature at a fixed mass flux on HTC (heat transfer coefficient).

similar trend with the change of specific heat according to the temperature. The temperature of CO_2 with the maximum HTC accords with the psuedocritical temperature with the maximum specific heat. In the above two trends, HTC during gas-cooling process is seen to be substantially affected by the thermodynamic properties.

Figure 3 shows the effects of operating temperature on HTC for various inlet pressures at the fixed mass flux of CO_2. In all of the pressure conditions, the HTC in the gas-cooling process gradually increases with decreasing temperature, has the maximum value nearby critical point, and then decreases. At the maximum HTC, the temperature of CO_2 nearly accords with the psuedocritical temperature as same as the maximum value of the specific heat. The maximum HTC becomes lower as the inlet pressure is increased while the average HTC is increased. When the pressure is increased from 7 to 10 MPa, average HTC is improved 14 to 50%.

Figure 4 shows the average HTC as a function of mass flux for various operating pressures. Average HTC is improved with increas-

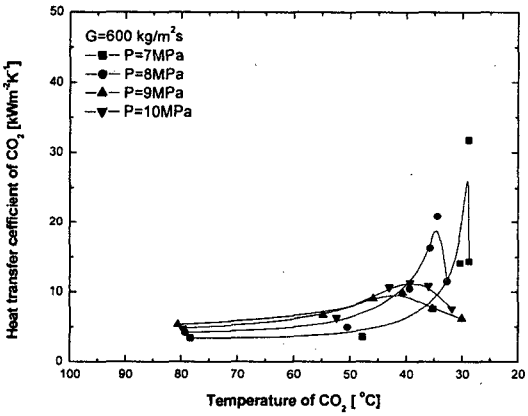

(a) 4.15 mm inner diameter tube

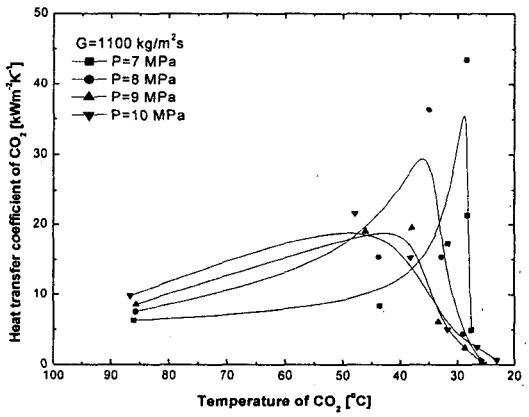

(a) 2.18 mm inner diameter tube

Fig. 3 Effects of operating temperature on HTC for various inlet pressures at a fixed mass flux of CO_2.

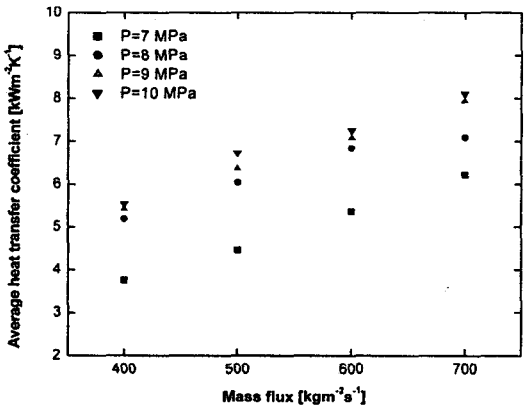

(a) 4.15 mm inner diameter tube

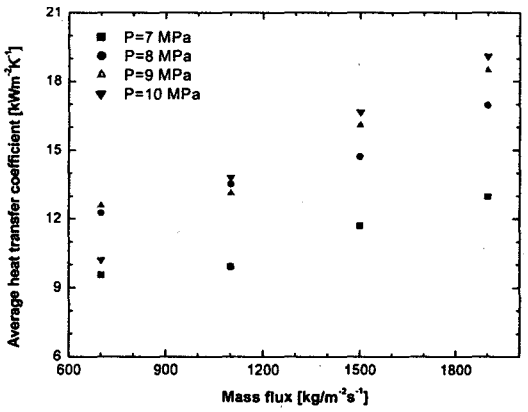

(b) 2.18 mm inner diameter tube

Fig. 4 Average HTC as a function of mass flux for various operating pressure.

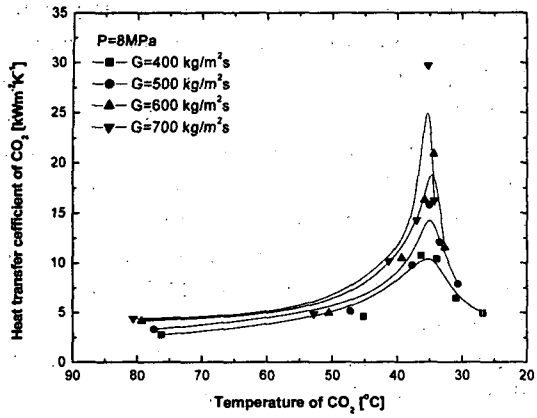

(a) 4.15 mm inner diameter tube

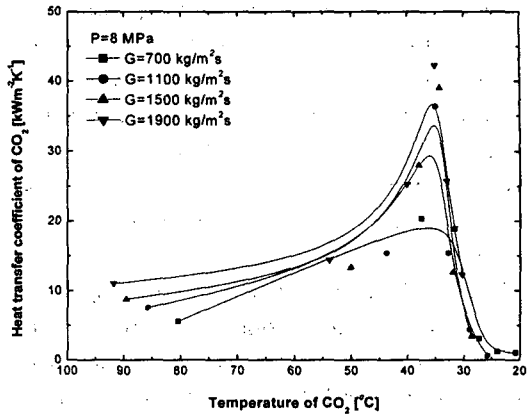

(b) 2.18 mm inner diameter tube

Fig. 5 Effects of operating temperature on HTC for various mass fluxes at a fixed operating pressure.

ing mass flux. When the mass flux is increased from 400 to 700 kg/m^{2}s for case 1 and 700 to 1,900 kg/m^{2}s for case 2, enhancement rate of average HTC was 16 up to 65% and 4 ~48%, respectively. When the mass flux condition of 700 kg/m^{2}s is constant and inner diameter of CO2 tube is changed 4.15 mm to 2.18 mm, enhancement rate of average HTC was 26 up to 72%. And when the similar mass flow rate condition of 5.42 g/s (case 1) and 5.60 g/s (case 2), average HTC is improved 180 up to 200%. At this time, mass flux condition is changed 400 kg/m^{2}s for case 1 to 1,500 kg/m^{2}s for case 2.

Figure 5 shows the effects of operating temperature on HTC for various mass fluxes of CO2 at the fixed pressure. As seen in this figure, the increase of the mass flux improves the HTC because the Reynolds number increases with increasing flow velocity, as expected. And heat transfer enhancement nearby pseudocritical temperature is much greater than that at other temperature ranges.

3.2 Pressure drop characteristics

Figure 6 shows pressure drop characteristics during gas-cooling process for various mass

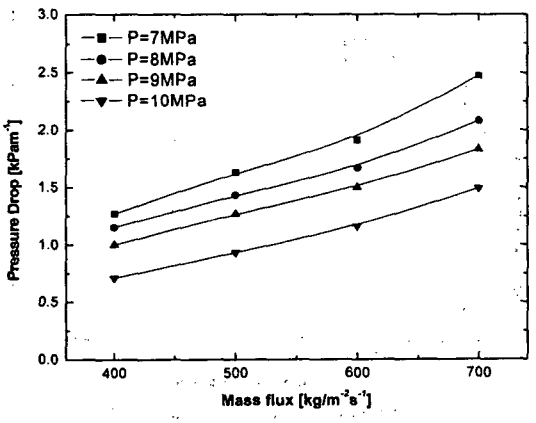

(a) 4.15 mm inner diameter tube

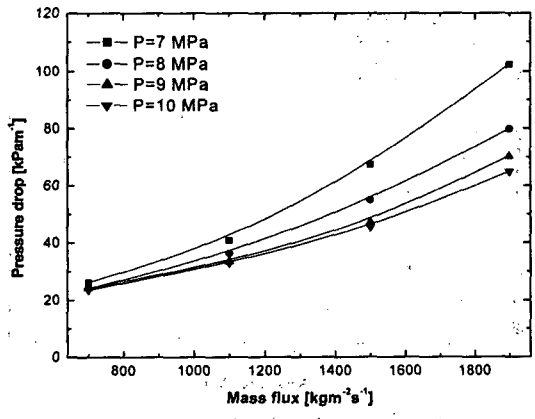

(b) 2.18 mm inner diameter tube

Fig. 6 Effects of mass flux on pressure drop for various operating pressure.

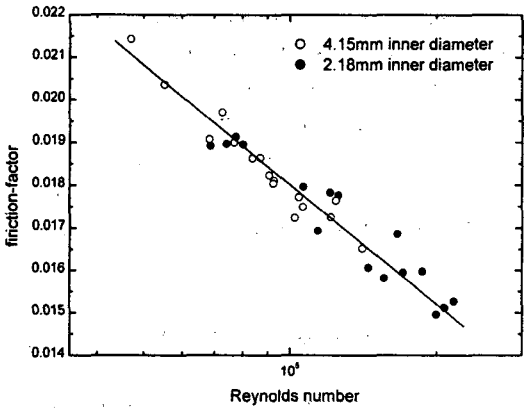

Fig. 7 Comparison of experimental data with Filonenko's f-factor correlation.

fluxes and inlet pressures. As the mass flux is increased, the pressure drop is also increased. And the pressure drop is decreased at higher operating pressure because of increasing density.

Figure 7 shows the friction factor for various Reynolds numbers. It was nearly corresponding with Filonenko's friction factor correlation [10] that is widely used for the turbulent flow in a smooth tube as shown in Eq. (8).

$$f=(1.82\log \mathrm{Re}-1.64)^{-2} \quad (1\times10^{4}\le \mathrm{Re}\le 5\times10^{6}) \quad (8)$$

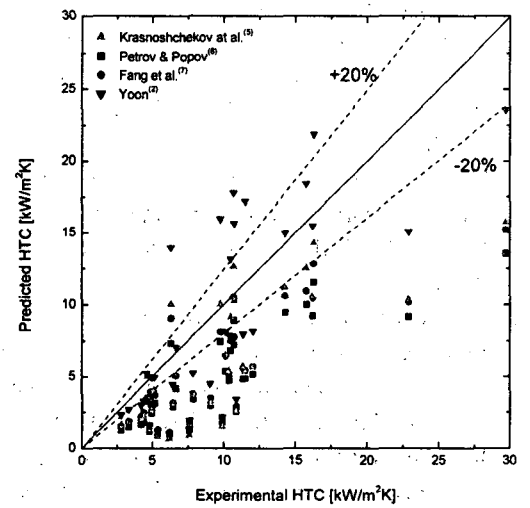

Fig. 8 Comparison between previous correlations and measured HTC.

3.3 Heat transfer correlation

Figure 8 shows the comparison between previous correlations[2,5-7] and measured HTC. Predicted HTC by previous correlations is smaller than experimental HTC. Among these correlations, Fang's correlation predicted the similar tendency to the measured HTC. Accordingly, in the present study a new correlation is proposed in a modified form of Fang's correlation, for the heat transfer during gas-cooling process in the horizontal tube as shown in Eq. (9). This correlation is based on Gnielinski's correlation, and includes thermodynamic properties, the specific heat and the enthalpy, which affect HTC.

$$\mathrm{Nu}_w = A_1 \frac{(f_w/8)(\mathrm{Re}_w-1000)\mathrm{Pr}_w}{A_2+12.7(f_w/8)^{1/2}(\mathrm{Pr}_w^{2/3}-1)} \times\left(1-0.001\frac{q_w}{G}\right)\left(\frac{\overline{c_p}}{c_{p_w}}\right)^{n} \quad (9)$$

$A_1=1.69$ for 4.15 mm inner diameter tube
$A_2=1.34$ for 2.18 mm inner diameter tube

Here, f_w is calculated by Churchill's correlation, evaluated at T_w, as shown in Eq. (10). And

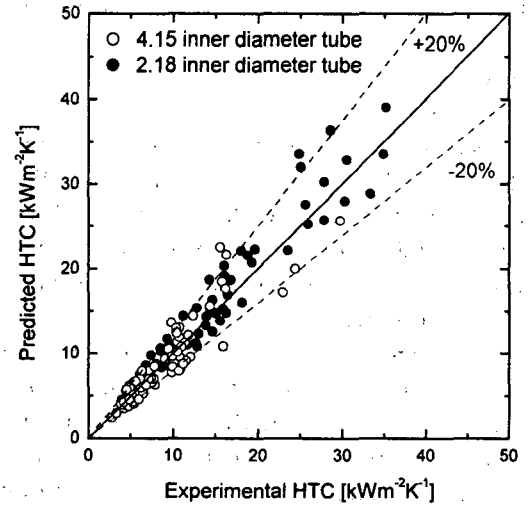

Fig. 9 Comparison between proposed correlation and measured HTC.

A_2, $\overline{c_p}$, and n are calculated by Eqs. (11), (12), and (13), respectively.

$$f_w = 8\left[\left(\frac{8}{\mathrm{Re}_w}\right)^{12} + \left\{\left(2.457\ln\frac{1}{(7/\mathrm{Re}_w)^{0.9}+0.27R_{rt}}\right)^{16} + \left(\frac{37530}{\mathrm{Re}_w}\right)^{16}\right\}^{-3/2}\right]^{1/12} \quad (10)$$

$$A_2 = \begin{cases} 1+7\times10^{-8}\mathrm{Re}_w & \mathrm{Re}_w < 10^6 \\ 1.07 & \mathrm{Re}_w \geq 10^6 \end{cases} \quad (11)$$

$$\overline{c_p} = \frac{i_m - i_w}{T_m - T_w} \quad (12)$$

$$n = 0.9 - 4\times10^{-4}(q_w/G) \quad (13)$$

Figure 9 shows the comparison between proposed correlation and measured HTC. The proposed correlation can predict heat transfer coefficient within the error of 20% on experimental conditions.

4. Conclusions

The experiments have been carried out to investigate the heat transfer coefficient and the pressure drop during critical and supercritical gas-cooling process of CO_2 in the horizontal tube.

The HTC of CO_2 is increased gradually with a decrease in the operating temperature during the gas-cooling process. And then, the HTC decreases after reaching the maximum value at near critical region. At this time, the maximum HTC accords with pseudocritical temperature of CO_2. The maximum HTC becomes lower as the inlet pressure is increased. The HTC improves with the mass flux of CO_2 and the heat transfer enhancement nearby pseudocritical temperature is much greater than that at other temperature ranges. Average HTC improves with an increase in the mass flux and pressure.

The pressure drop is increased with an increase in the mass flux and is decreased with an increased the inlet pressure of CO_2. The friction factor is predicted well with Filonenko's correlation. The new correlation of heat transfer coefficient is proposed from a modified Fang's correlation and predicts within the error of 20%.

Acknowledgement

This work was supported by Next-Generation-Technology R&D program of the Ministry of Commerce, Industry and Energy, Korea.

References

1. Hwang, Y. and Radermacher, R., 1999, Experimental investigation of the CO_2 refrigeration cycle, ASHRAE Trans., Vol. 105, Part 1, Paper No. CH-99-22-2.
2. Yoon, S. H., 2002, Studies on the characteristics of evaporation and supercritical gas cooling heat transfer of carbon dioxide, Ph. D. Thesis, Seoul National University, Seoul, Korea.
3. Yin, J. M., Bullard, C. W. and Hrnjak, P. S., 2000, Design strategies for R744 gas cooler, Preliminary Proceedings of the 4th IIR-Gustav Lorentzen Conference on Natural Working Fluids at Purdue, July 25-28, USA, pp. 315-322.
4. Hwang, Y. and Radermacher, R., 1998, Theoretical of carbon dioxide refrigeration cycle, Int. J. HVAC&R Research, Vol. 4, No. 3, pp. 245-263.
5. Krasnoshchekov, E. A., Kuraeva, I. V. and Protopopov, V. S., 1970, Local heat transfer of carbon dioxide at supercritical pressure under cooling conditions, High Temperature Institute (Translated from Teplofizika Vysokikh Temperatur), Vol. 7, No. 5, pp. 856-862.
6. Petrov, N. E. and Popov, V. N., 1985, Heat transfer and resistance of carbon dioxide be-

ing cooled in the supercritical region, Thermal Engineering, Vol. 32, No. 3, pp. 131-134.
7. Fang, X., Bullard, C. W. and Hrnjak, P. S., 2001, Modeling and analysis of gas coolers, ASHRAE Trans., Vol. 107, Part 1, Paper No. 4411.
8. Olsen, D. A., 2000, Heat transfer of supercritical carbon dioxide flowing in a cooled horizontal tube, Preliminary Proceedings of the 4th IIR-Gustav Lorentzen Conference on Natural Working Fluids at Purdue, July 25-28, USA, pp. 251-258.
9. Pitla, S. S., Groll, E. A. and Ramadhyani, S., 2001, Convective heat transfer from in-tube cooling of turbulent supercritical carbon dioxide: Part 2-Experimental data and numerical predictions, Int. J. HVAC&R Research, Vol. 7, No. 4, pp. 367-382.
10. Incropera, F. P. and DeWitt, D. P., 1990, Introduction to Heat Transfer, 2nd ed., John Wiley & Sons, New York, pp. 455-460.